Impact of Proton Irradiation on the Static and Dynamic Characteristics of High-Voltage 4H-SiC JBS Switching Diodes

Zhiyun Luo, *Student Member, IEEE*, Tianbing Chen, *Student Member, IEEE*, John D. Cressler, *Fellow, IEEE*, David C. Sheridan, *Member, IEEE*, John R. Williams, Robert A. Reed, *Member, IEEE*, and Paul W. Marshall, *Member, IEEE*

***Abstract*—The effects of proton irradiation on the static (*dc*) and dynamic (switching) performance of high-voltage 4H-SiC Junction Barrier Schottky (JBS) diodes are investigated for the first time. In contrast to that observed on a high-voltage Si *p – i – n* diode control device, these SiC JBS devices show an increase (degradation) in series resistance (R_S), a decrease (improvement) of reverse leakage current, and increase (improvement) in blocking voltage after high-fluence proton exposure. Measured breakdown voltages of post-irradiated SiC diodes increase on average by about 200 V after irradiation. Dynamic reverse recovery transient measurements show good agreement between the various *dc* observations regarding differences between high-power SiC and Si diodes, and show that SiC JBS diodes are very effective in minimizing switching losses for high-power applications, even under high levels of radiation exposure.**

***Index Terms*—Diode, junction barrier Schottky (JBS), proton radiation, Schottky barrier diodes (SBD), silicon carbide (SiC).**

TABLE I
POWER SEMICONDUCTOR MATERIAL PARAMETERS

Material	Si	GaAs	4H-SiC	6H-SiC
E_G	1.12	1.42	3.23	3.03
n_i	$1x10^{10}$	$1.8x10^{10}$	$5x10^{-9}$	$1.6x10^{-6}$
μ_n(cm^2/V·s)	1350	8500	650	370
$\mu_{//}$			370	50
E_C (MV/cm)	0.3	0.4	2.0	2.4
V_{sat} (10^7)	1.0	2.0	2.0	2.0
λ (W/cm·s)	1.5	0.5	4.5	4.5
BFOM	1	15.6	130	110

I. INTRODUCTION

SILICON carbide (SiC) is a promising candidate for high-power and high-frequency applications because of its wide bandgap (> 3 eV) and excellent thermal/electrical properties [1]. Table I lists some important semiconductor material parameters for power device applications. Compared to Si, SiC enjoys an order of magnitude improvement in critical field strength (E_C), twice the saturation velocity ($V_{\rm sat}$), and three times the thermal conductivity (λ). Baliga's figure-of-merit (BFOM) [2] suggests that SiC should have more than an order of magnitude theoretical advantage over Si for unipolar power devices. SiC-based devices are very attractive for military and space-based power electronics systems mainly due to their fast switching speeds compared to Si, their low switching losses, and their ability to operate in extreme environments such as high temperature (e.g., to 500°C) and/or under high levels of radiation. The radiation literature on SiC devices is very limited, and studies to date have been centered on terrestrial detector systems. 4H-SiC neutron detectors, for instance, have been demonstrated with no significant degradation of detection efficiency after neutron fluences up to 1×10^{17} n/cm^2 [3]. Devices based on 6H-SiC have shown negligible degradation of device characteristics for gamma radiation doses up to 100 Mrad, but showed significant degradation with neutron irradiation for fluences in excess of 1×10^{16} n/cm^2 [4], [5].

In earlier studies, the effects of high-dose gamma irradiation on unterminated 4H-SiC Schottky diodes and the *SiC* – SiO_2 interface was examined [6], and no observable degradation in the diode forward and reverse characteristics up to a total dose of 4 Mrad(Si) was observed. Measured breakdown voltages of post-irradiated diodes increased, however, approximately 200 V after irradiation, an improvement attributed to a radiation-induced increase in negative interface charge. In the present work, we present for the first time the effects of proton irradiation on both the *dc* and *ac* characteristics of terminated 4H-SiC high-voltage JBS power switching diodes. JBS diodes have been shown to have great promise for power switching systems, since they effectively balance the best properties of both Schottky Barrier Diodes (SBD) (high speed) with *pn* junction diodes (low leakage currents and hence losses). A comparison is made to commercially-available high-voltage Si *p – i – n* power diodes in order to better understand the results.

Manuscript received July 16, 2003; revised September 23, 2003. This work was supported by NASA Cooperative Agreement NCC8-237, NASA Grant NAG3-2639, the Auburn University CSPAE, DTRA under the Radiation Tolerant Microelectronics Program, and NASA-GSFC under the Electronics Radiation Characterization Program.

Z. Luo is with the Alabama Microelectronics Science and Technology Center, Electrical and Computer Engineering Department, Auburn University, Auburn, AL 36849 USA (e-mail: lozhiyu@eng.auburn.edu).

T. Chen and J. D. Cressler are with the School of Electrical and Computer Engineering, Georgia Institute of Technology, Atlanta, GA 30332 USA.

D. C. Sheridan is with IBM Microelectronics, Essex Junction, VT 05452 USA.

J. R. Williams is with the Physics Department, Auburn University, Auburn, AL 36849 USA.

R. A. Reed is with NASA-GSFC, Code 562, Greenbelt, MD 20771 USA.

P. W. Marshall is a consultant to NASA-GSFC, Greenbelt, MD 20771 USA.

Digital Object Identifier 10.1109/TNS.2003.821806

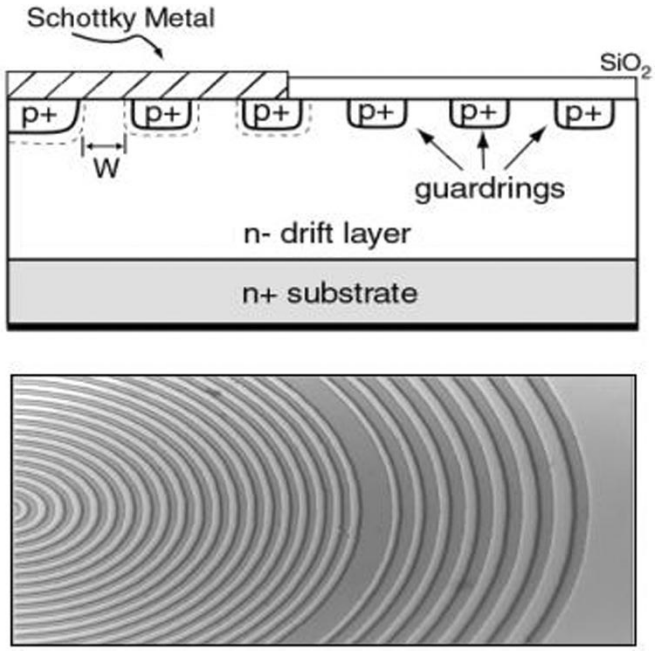

Fig. 1. SiC JBS structure with floating guard ring edge termination.

II. Experiment

Circular SBD and JBS diodes with diameters ranging from 100 μm to 400 μm were fabricated at Auburn University on 4H-SiC n+ wafers having a 30 μm thick 1×10^{15} cm^{-3} n- epitaxial layer grown at Cree, Inc. The active JBS regions, together with the floating guard ring structures needed for proper edge termination, were formed using Al (i.e., p-type) implantation at high temperatures. The guard rings as well as p^+ implants used in forming the JBS active region were 5 μm in width, while the JBS ring-to-ring spacing (W) varied from 3 μm to 5 μm. Al implants were annealed at 1600°C, as has been described in the literature [7]. The guard ring-to-guard ring spacing and number for a given device design was chosen after extensive calibrated quasi 3-D simulations to optimize the breakdown properties of the device in question. A high quality thermal oxide followed by a 1 μm poly-Si layer, which was then converted to oxide, was used for surface passivation. Ni was deposited for the backside ohmic contacts and annealed at 1100°C for 2 min in vacuum, followed by evaporation of Ti and Au for decreased contact resistance. Schottky contact openings were formed by selective RIE followed by a BOE etch through the passivation and immediate loading into the metallization chamber for Ni Schottky contact evaporation. Schottky contacts were completed with Ti and Au overlayers. The thickness of Ni, Ti, and Au were 120, 150, and 80 nm respectively. A schematic cross-section and top-down photograph of the fabricated JBS diodes is shown in Fig. 1. the SBD diodes have identical structures to JBS diodes except that there is no p+ regions under the Schottky contact.

Proton irradiation of the SiC SBD, SiC JBS, and the packaged commercial Si $p-i-n$ control diode (UF1007) was performed at the Crocker Nuclear Laboratory Cyclotron Facility, University of California at Davis, using 62.5 MeV protons, to a total fluence of 5×10^{13} $\mathrm{p/cm}^2$, with terminals floating. We tested over 50 samples on three different dies of 4H-SiC diodes

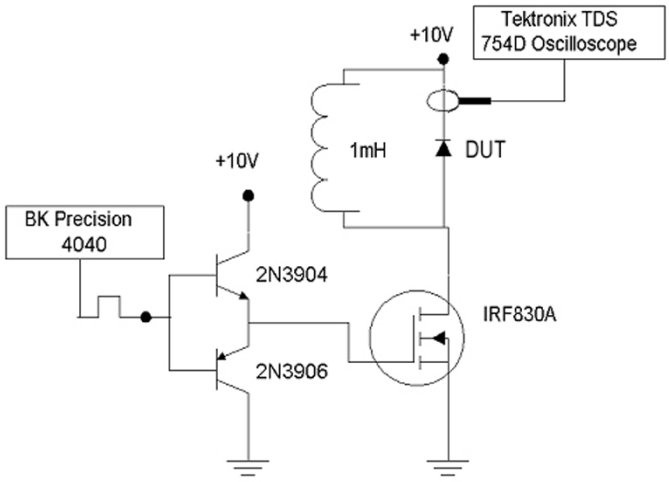

Fig. 2. Schematic of the test circuit used in the reverse recovery transient measurements.

both before and after proton irradiation to ensure enough results for analysis. Both *dc* and *ac* characteristics were measured and compared. The low-voltage forward and reverse current-voltage characteristics were measured using an Agilent 4155 Semiconductor Parameter Analyzer. Reverse breakdown measurements were performed using a Tektronix 371 high voltage curve tracer. For reverse recovery measurements, the inductive switching test circuit shown in Fig. 2 was used. In this test circuit, the device-under-test (DUT) is connected as a "freewheeling" diode in parallel with an inductive load. This circuit is designed to provide a dI_r/dt of -10 $\mathrm{A}/\mu\mathrm{sec}$.

III. Results and Discussion

A. dc Characteristics

Fig. 3 shows typical forward *dc* characteristics of a JBS diode with 3 μm JBS ring spacing and seven guard ring termination, both before and after 5×10^{13} $\mathrm{p/cm}^2$ irradiation. As is widely known, adequate edge termination is critical in power devices in order to minimize field crowding at the device edges and hence maximize breakdown voltage [2]. The termination structure used here employs multiple floating guard ring structures carefully optimized via calibrated simulations, and has proven to be very effective at providing sufficient termination without enhancing processing complexity [8].

The low-injection region of the $J-V$ curve shows little change after irradiation, suggesting that proton exposure does not degrade the Schottky contact of the device (i.e., the barrier remains unchanged at 0.94 eV). In addition, however, the forward voltage drop clearly increases at higher currents due to proton-induced series resistance. The series resistance (R_s) increases dramatically in the case of the JBS diode shown, from 25 Ω (pre-rad) to 12.1 $\mathrm{M}\Omega$ (post-rad). Our Previous research showed little or no degradation of R_s after gamma irradiation, even up to 100 Mrad total dose, which suggests that SiC device behavior depends strongly on the radiation type. Our results are repeatable, however, across many devices on separate samples, indicating that the effect is real. The source of the added resistance after irradiation is either due to: 1) added contact resis-

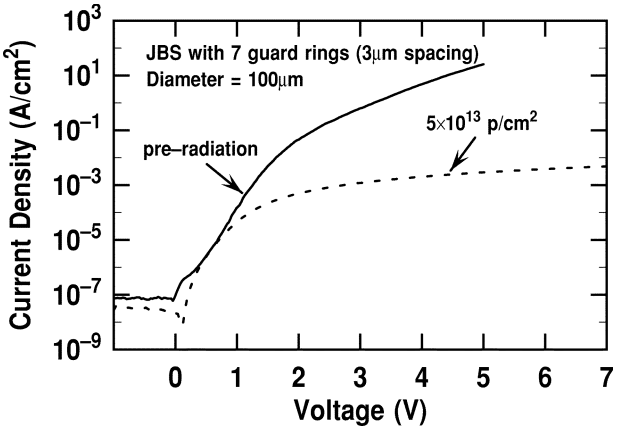

Fig. 3. Forward current-voltage characteristics of the seven guard ring terminated 4H-SiC JBS diode, before and after proton exposure. Inset: enlarged J-V characteristics of the seven guard ring terminated 4H-SiC JBS and SBD diodes (100 μm diameter), before and after proton exposure.

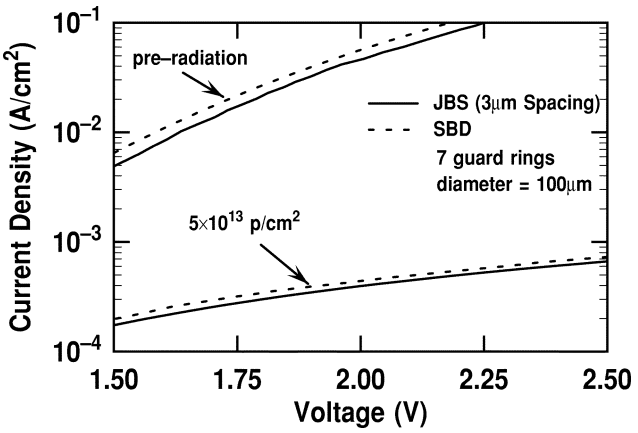

Fig. 4. Enlarged forward current-voltage characteristics of the terminated 4H-SiC JBS and SBD diodes, before and after proton exposure.

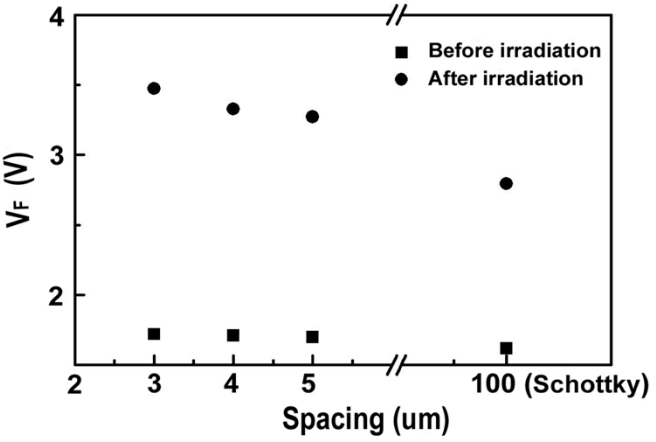

Fig. 5. Forward voltage drop as a function of guard ring numbers for SiC diodes before and after proton exposure.

tance from the metal itself; 2) a decrease in substrate doping level due to carrier removal by proton-induced charge trapping [9], [10]; or 3) a radiation-induced change in the carrier mobility due to cattering of the carrier by the charged traps, or a combination of the three. In order to eliminate potential contact resistance changes, we remeasured the J-V characteristics of the JBS diode using a Kelvin contact (i.e., force bias on one probe and measure on the other probe) in order to eliminate contact resistance, obtaining in this case $R_s = 7.2\ \mathrm{M}\Omega$. A measurement of resistance of the metal itself shows an increase from 5–15 Ω for pre-radiation samples to 1.2–2.2 kΩ for post-radiation samples. The relative resistance change of the metal suggests that proton exposure has changed the surface chemistry of the metal, but clearly does not explain the total resistance change. Displacement damage can also de-ionize dopant impurities and/or introduce traps into the SiC epi, thereby leading to an increase in series resistance from the bulk of the wafer [11]–[13]. From the $C-V$ measurements on the SBD, we obtained 2–5 $\times 10^{14}\ \mathrm{cm}^{-3}$ epi effective doping level, down from a starting value of 1–2 $\times 10^{15}\ \mathrm{cm}^{-3}$ in the active region of the device (i.e., reverse bias can only probe a finite volume of the wafer). The carrier removal rate is 10–16 /cm calculated from C-V results. This suggests that proton-induced dopant de-ionization also plays a role in the resistance increase after proton exposure.

Fig. 4 is the enlarged portion of the J–V characteristics of the same JBS diode from 1.5 to 2.5 V, comparing it to a standard terminated SBD diode. Both SBD and JBS diodes present similar forward-bias performance, before and after radiation. To show the influence of the p+ region on the radiation response, the forward voltage drop at fixed current density ($10^{-3}\ \mathrm{A/cm}^2$) for different spacings before and after irradiation is shown in Fig. 5. The voltage drops after irradiation are much higher than those before irradiation for different spacings of the JBS structure. Also of note is a more obvious increase of forward voltage drop as the spacing decreases for the post-radiation diodes. This is due to the decrease of effectiveness of JBS structure itself. That is, the effective epi doping change leads to a decrease of the active area and, thus, decreases the effectiveness of current collection under forward current flow. This is not unexpected because as the effective doping in the active region decreases, the depletion region of the p-n structure expands. Thus, the effective area of the Schottky contact region is smaller, leading to higher forward voltage drop and a severe series resistance increase. MEDICI simulations were used to confirm this analysis. According to the simulations, the current at high injection showed a decrease of almost two orders of magnitude with a doping change from 1×10^{15} to $2 \times 10^{14}\ \mathrm{cm}^{-3}$ for these JBS structures. For an ideal Schottky diode, however, the decrease is within one order of magnitude. However, all of the SBDs in this study (only 100 μm diameter) also show a strong increase of forward voltage after irradiation. This difference is actually a result of the contribution from the p+ edge termination. That is, if the SBD is a small diode with guard rings at the edge, the influence of the p+ guard ring can also cause a dramatic decrease of high injection current. Thus, we can conclude that at low doping, the JBS structure is not as effective at improving forward current-voltage characteristics. For small diodes, the influence of p+ edge termination to the I-V characteristics of these diodes is more significant. For comparison to these SiC results, Fig. 6 shows the $I-V$ characteristics of the commercial Si *p–i–n* diode (area and type of termination structure are

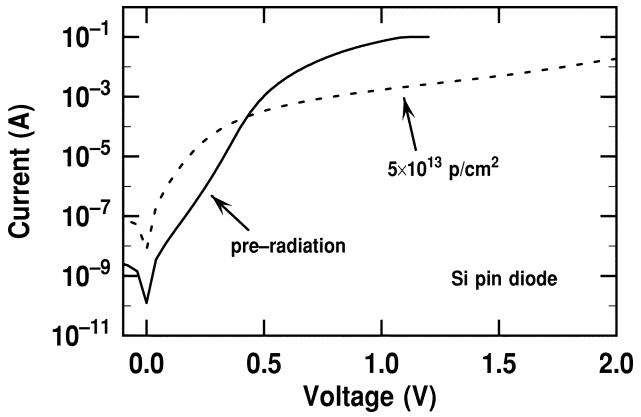

Fig. 6. Forward current-voltage characteristics of the Si *p–i–n* diode before and after proton exposure.

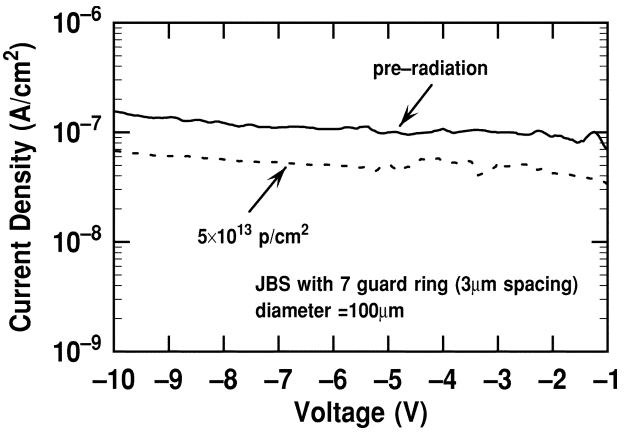

Fig. 7. Reverse current-voltage characteristics of the terminated 4H-SiC JBS diode before and after proton exposure.

unknown). The Si *p–i–n* diode shows much stronger degradation in the low-bias region, consistent with G/R center production and lifetime changes in the device epi region. Interestingly, we also see a significant series resistance increase after proton exposure, presumably also due to dopant de-ionization.

A surprising result is that we consistently observe a *decrease* in the reverse current of the SiC diodes after radiation (Fig. 7), which is opposite to the (expected) degradation observed in the Si diode (Fig. 8). The reverse current density of the SiC diodes decreases from 1.6×10^{-7} A/cm^2 to 7×10^{-8} A/cm^2 at 10 V. For the Si diodes, on the other hand, the current dramatically increases from 6.8×10^{-9} A to 1.4×10^{-7} A at 10 V, consistent with radiation-induced G/R center production and hence lifetime reduction. For the SiC devices, this result is actually consistent with an earlier report using *EBIC*, which indicated that electron irradiation can have a pronounced annealing effect on carrier lifetime in 6H-SiC epi [16], although this has not been observed to our knowledge using protons. Low effective doping level due to carrier removal effect of proton irradiation also could also influence the reverse current at low reverse voltage, since the JBS diode has wider depletion area in the junction at the same voltage, resulting in a smaller Schottky contact area. This is important especially at low reverse voltage, given that the Schottky area could still contribute leakage current at low reverse voltage.

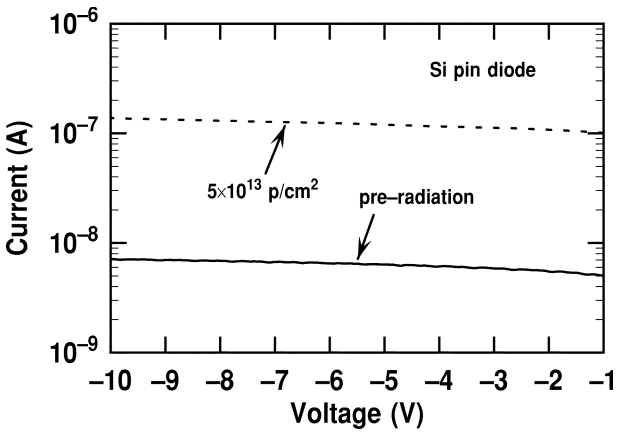

Fig. 8. Reverse current-voltage characteristics of the Si *p–i–n* diode before and after proton exposure.

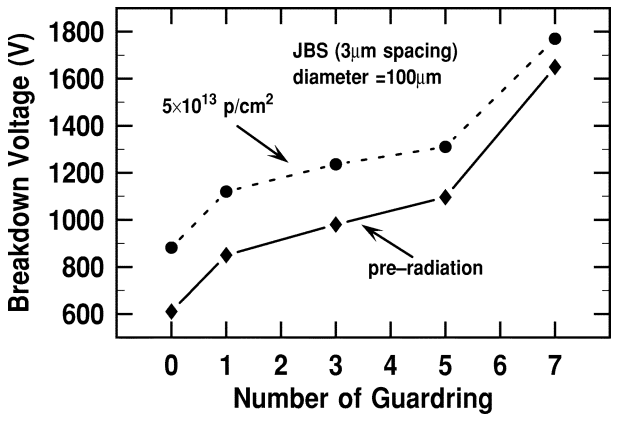

Fig. 9. Comparison of measured breakdown voltage of the JBS diode between pre- and post-irradiation as a function of number of guard rings used in the edge termination.

We have observed that the breakdown voltage actually increases in these SiC JBS diodes after proton exposure, which is similar to what have been observed in Si detectors after neutron irradiation [17]. This is one of a few instances when radiation actually improves device characteristics. For the Si p-i-n diode, however, the breakdown voltage has no obvious change and remains around 1300 V. Fig. 9 shows the radiation-induced change in breakdown voltage as a function of number of guard rings used in the termination structure of the SiC diodes. The average increase in breakdown voltage is 220 V, a significant improvement. Clearly, the effect is not strongly dependent on the number of rings, although a gradual saturating trend at high guard ring count is apparent. A peak blocking voltage in this technology of 1780 V after 5×10^{13} p/cm^2 exposure is achieved.

We have previously observed a similar breakdown voltage increase in unterminated SiC SBD diodes after gamma radiation and attributed that to an increase of negative surface charge in the SiO_2/SiC passivation layer [6], [18]. A negative surface charge increases the depletion layer spreading, thus reducing the effects of field crowding at the device edge, and thereby increasing the breakdown voltage. Given the similar observed trends in the blocking voltage, a similar explanation is certainly plausible here, even though the radiation type is different. In addition, however, we note that the dopant de-ionization needed to explain the series resistance increase

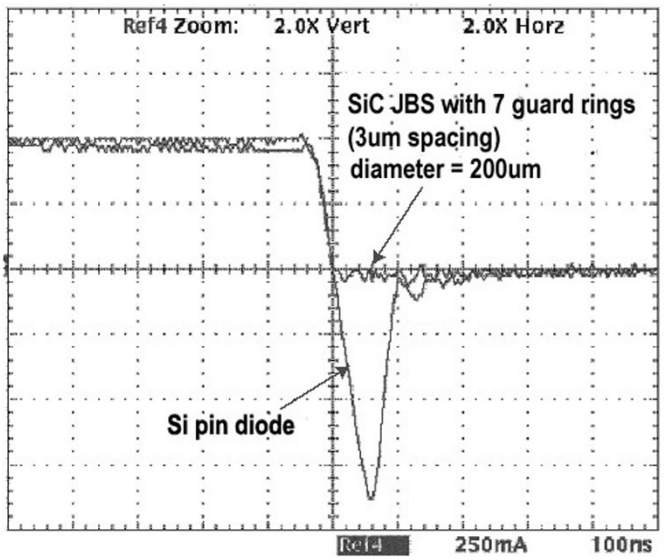

Fig. 10. Reverse recovery transient waveforms comparing the SiC JBS and Si *p–i–n* diodes.

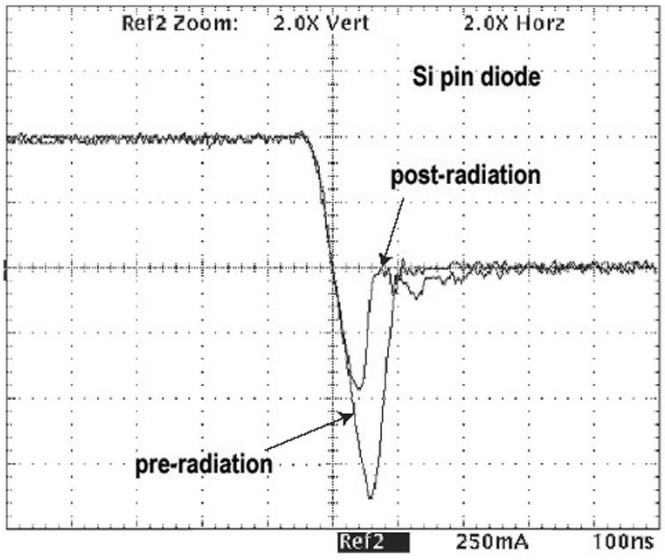

Fig. 11. Reverse recovery transient waveforms comparing the pre- and post-irradiated Si *p–i–n* diode.

would also improve the breakdown voltage, and thus it is likely that a combination of both effects in operative here. Using calibrated MEDICI simulations [19], the breakdown voltage for the planar diode structure was calculated for both surface charge changes as well as doping level changes. The simulation results suggest that a doping change from $1 \times 10^{15}\ \mathrm{cm}^{-3}$ to $7 \times 10^{14}\ \mathrm{cm}^{-3}$ would cause a 200 V breakdown increase, while a negative charge change increase from $-1.67 \times 10^{-12}\ \mathrm{cm}^{-2}$ to $-3.24 \times 10^{-12}\ \mathrm{cm}^{-2}$ would cause a similar increase. Further experiments involving proton exposure of MOS capacitors will be needed to sort this out and is presently underway.

B. Switching Characteristics

SiC JBS diodes have a negligible reverse recovery current compared to Si *p–i–n* diodes, greatly improving their losses for high-power switching circuits (Fig. 10). In the Si *p–i–n* structure, the observed reverse recovery current is primarily due to minority carrier storage (set by the carrier lifetime). The JBS diode, however, is a majority carrier device (like the SBD), and hence has negligible carrier storage under high-injection currents. As shown in Fig. 10 for pre-radiation, the Si *p–i–n* diode has a reverse recovery current peak ($I_{rr,\max}$) of 930 mA and reverse recovery time (t_{rr}) of 101 ns, while for the SiC JBS diode, $I_{rr,\max}$ is only 62 mA and with a t_{rr} of 38 ns.

After radiation, the Si *p–i–n* diode yields a significantly decreased reverse recovery current, as shown in Fig. 11. Both $I_{rr,\max}$ and t_{rr} dramatically decrease from 930 mA and 101 ns to 480 mA and 69 ns. This indicates that the minority lifetime strongly decreases after proton exposure, consistent with our reverse leakage current observations. Similarly, electron radiation has been shown to strongly decrease the carrier lifetime in Si power devices [20]. As expected, for the SiC diodes, there is little change after irradiation, although we do still see a trend of increased $I_{rr,\max}$ and t_{rr} with proton exposure. For the particular terminated SiC JBS diode shown in Fig. 12, $I_{rr,\max}$ remains the same at 62 mA while t_{rr} increased from 38 to 44 ns after proton exposure. These reverse recovery transient

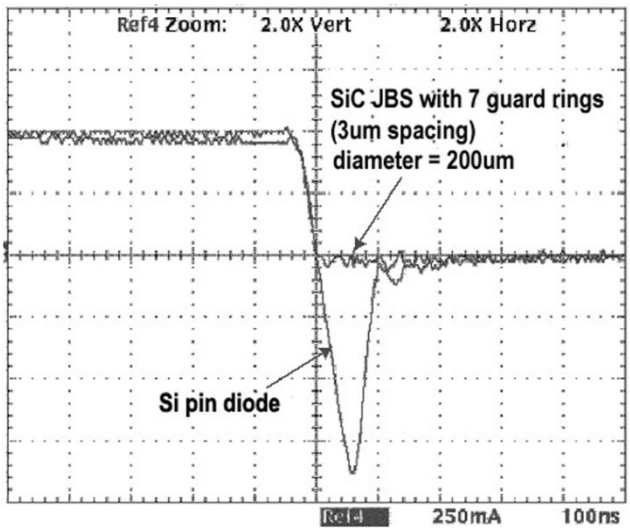

Fig. 12. Reverse recovery transient waveforms comparing the pre- and post-irradiated SiC JBS diode.

measurements are obviously low-voltage measurements, and more detailed ac characterization at higher di_{rr}/dt, and at full blocking voltage will need to be made, and is presently underway.

IV. Summary

The effects of proton irradiation on the static and dynamic performance of high-voltage 4H-SiC JBS diodes have been investigated for the first time. In contrast to that observed on a high-voltage Si *p–i–n* diode control device, these SiC JBS devices show an increase (degradation) in series resistance, a decrease (improvement) of reverse leakage current, and increase (improvement) in blocking voltage after high-fluence proton exposure. Dynamic reverse recovery transient measurements shows good agreement between the various *dc* observations regarding differences between high-power SiC and Si diodes, and show that SiC JBS diodes are very effective

in minimizing switching losses for high-power applications, even under high levels of radiation exposure.

ACKNOWLEDGMENT

The authors would like to thank T.F. Isaacs-Smith for insightful discussions on measurement techniques, C. Ellis for fabrication support, as well as L. Cohn and H. Brandhorst for their support of this work.

REFERENCES

[1] M. Bhatnagar and B. J. Baliga, "Comparison of 6H-SiC, 3C-SiC, and Si for power devices," *IEEE Trans. Electron Devices*, vol. 40, pp. 645–655, Mar. 1993.

[2] B. J. Baliga, *Power Semiconductor Devices*. Boston, MA: PWS, 1996.

[3] S. Seshadri, A. R. Dulloo, F. H. Ruddy, J. G. Seidel, and L. B. Rowland, "Demonstration of an SiC neutron detector for high-radiation environments," *IEEE Trans. Electron Devices*, vol. 46, pp. 567–571, June 1999.

[4] J. McGarrity, F. McLean, W. DeLancey, J. Palmour, C. Carter, J. Edmond, and R. Oakley, "Silicon carbide JFET radiation response," *IEEE Trans. Nuclear Science*, vol. 39, pp. 1974–1981, Dec. 1992.

[5] T. Ohshima, M. Yoshikawa, H. Itoh, Y. Aoki, and I. Nashiyama, "g-Ray irradiation effects on 6H-SiC MOSFET," *Mater. Sci. Eng. B*, vol. 61–62, pp. 480–484, 1999.

[6] D. C. Sheridan, G. Chung, S. Clark, and J. D. Cressler, "The effects of high-dose gamma irradiation on high-voltage 4H-SiC Schottky diodes and the SiC-SiO_2 interface," *IEEE Trans. Nucl. Sci.*, vol. 48, pp. 2229–2232, Dec. 2001.

[7] S. E. Saddow, M. Capano, J. A. Cooper, M. S. Mazzola, J. Williams, and J. B. Casady, "High temperature implant activation in 4H and 6H-SiC in a silane ambient to reduce step bunching," *Mater. Sci. Forum*, vol. 338–342, p. 901, 1999.

[8] D. C. Sheridan, G. Niu, J. N. Merrett, J. D. Cressler, C. Ellis, and C. C. Tin, "Design and fabrication of planar guard ring termination for high-voltage SiC diodes," *Solid-State Electron.*, vol. 44, pp. 1367–1372, 2000.

[9] G. C. Messenger, "A summary review of displacement damage from high enerry radiation in silicon semiconductors and semiconductor devices," *IEEE Trans. Nucl. Sci.*, vol. 39, pp. 468–473, June 1992.

[10] D. C. Sheridan, G. Niu, J. N. Merrett, J. D. Cressler, C. Ellis, and C. C. Tin, "Design and fabrication of planar guard ring termination for high-voltage SiC diodes," *Solid-State Electron.*, vol. 44, pp. 1367–1372, 2000.

[11] L. Storasta, F. H. C. Carlsson, S. G. Sridhara, D. Aberg, J. P. Bergman, A. Hallen, and E. Janzen, "Proton irradiation induced defects in 4H-SiC," *Mater. Sci. Forum*, vol. 353–356, pp. 431–434, 2001.

[12] H. J. von Bardeleben and J. L. Cantin, "Intrinsic defects in 6H-SiC generated by electron irradiation at the silicon displacement threshold," *Mater. Sci. Forum*, vol. 353–356, pp. 509–512, 2001.

[13] I. N. Makeeva, S. M. Okulov, T. L. Petrenko, T. T. Petrenko, and H. J. von Bardeleben, "EPR study of carbon vacancy-related defects in electron-irradiated 6H-SiC," *Mater. Sci. Forum*, vol. 353–356, pp. 517–520, 2001.

[14] A. M. Strelchuk, A. A. Lebedev, V. V. Kozlovski, N. Natali, S. Savkina, D. V. Davydov, V. V. Solov'ev, and M. G. Rastegaeva, "Doping of 6H-SiC pn structures by proton irradiation," *Nucl. Instrum. Methods Phys. Res. B*, vol. 147, pp. 74–78, 1998.

[15] D. C. Look and J. R. Sizelove, "Defect production in electron-irradiated n-type GaAs," *J. Appl. Phys.*, vol. 62, no. 9, pp. 3660–3664, 1987.

[16] W. A. Doolittle, A. Rohatgi, R. Ahrenkiel, D. Levi, G. Augustine, and R. Hopkins, "Understanding the role of defects in limiting the minority carrier lifetime in SiC," in *Proc. MRS Power Semiconductor Materials and Devices Symp.*, Boston, MA, 1997, pp. 197–202.

[17] S. M. Y. Hasan, S. L. Kosier, R. D. Schrimpf, and K. F. Galloway, "Effect of neutron irradiation on the breakdown voltage of power MOSFET's," *IEEE Trans. Nucl. Sci.*, vol. 41, pp. 2719–2726, Dec. 1994.

[18] T. Chen, Z. Luo, J. D. Cressler, T. F. Isaacs-Smith, J. R. Williams, G. Chung, and S. D. Clark, "The effects of NO passivation on the radiation response of SiO_2/4H-SiC MOS capacitors," *Solid-State Electron.*, vol. 46, no. 12, pp. 2213–2235, 2002.

[19] *MEDICI 2-D Semiconductor Device Simulator*, 4.3 ed., Avant! Corp., Palo Alto, CA, 1999.

[20] F. J. Niedernostheide, M. Schmitt, H. J. Schulze, U. Kellner-werdehausn, A. Frohnmeyer, and G. Wachutka, "Analysis of radiation-induced defects and performance conditioning in high-power devices," *J. Electrochem. Soc.*, vol. 150, no. 1, pp. 15–21, 2003.